JTTEE5 17:73–81
DOI: 10.1007/s11666-007-9147-z
1059-9630/$19.00 © ASM International

Peer Reviewed

Influence of Suspension Plasma Spraying Process Parameters on TiO_2 Coatings Microstructure

Roman Jaworski, Lech Pawlowski, Francine Roudet, Stefan Kozerski, and Agnès Le Maguer

(Submitted February 21, 2007; in revised form April 29, 2007)

The study aimed at optimizing the suspension plasma spraying of TiO_2 coatings obtained using different suspensions of fine rutile particles in water solution onto aluminum substrates. The experiments of spraying were designed using a 2^3 full factorial plan. The plan enabled to find the effects of three principal parameters, i.e. electric power input to plasma, spray distance, and suspension feed rate onto microstructure of coatings, content of anatase phase and size of anatase crystals in the coatings. The microstructure of deposits was observed with scanning electron microscope (SEM) and optical microscope and their composition was characterized using energy dispersive spectrometry (EDS). The observations were made on the coatings surface and their cross-sections. The latter made it possible to determine the coatings thicknesses to be in the range from 8 to 33 μm.

Keywords suspension plasma spraying, titania coatings, XRD phase analysis

1. Introduction

TiO_2 is a frequently used oxide, which can be used in, e.g. chemical, electronic and optical industries. The oxide may be applied as a thin film deposited by PVD or a thick coating obtained by thermal spraying (Ref 1, 2). The application of thermally sprayed coatings, which is about to emerge is a deposition of photocatalytic coatings (Ref 3-6). The photocatalytic activity seems to be promoted by the appropriate phase composition of coatings, which should possibly include anatase. The tested coatings have been prepared by vacuum or atmospheric plasma spraying of coarse powders and by atmospheric plasma spraying of fine precursors in suspension (Ref 3-6). Suspension plasma spraying has been applied recently to develop the nanostructural coatings (Ref 7). One of the first tested applications was a development of thermal barrier coatings (Ref 8, 9). The physics and chemistry of suspension spray processes were analyzed by Fauchais et al. (Ref 10). At the processing, the liquid feedstock containing fine particles is fed into plasma jet using a peristaltic pump or similar device (see Fig. 1). The suspension is fed to an atomizer and gets injected into plasma jet. The solid content in the atomized droplets starts to agglomerate, melt (some of them will vaporize) and eventually solidify in-flight before impacting on the substrate. The formation of anatase in suspension sprayed coatings was explained by the phenomena occurring at small droplet solidification (Ref 11). The explanation is based onto the calculation made by Li and Ishigaka (Ref 12), which show that at the temperature of solidus lower than 2075 K (melting point in equilibrium condition is equal to $T_m = 2143$ K), the nucleation of anatase occurs and above this temperature—that of rutile. Taking this model the nucleation of anatase would be favored mainly by the temperature at which nucleation from the melt begins and the rate of cooling down of solidified droplet. The latter, for fine particles used at suspension spraying, should depend on the operational processing parameters such as spray distance, electric power input to the torch, linear velocity of torch at spraying among others. The present study focuses on optimizing the spray conditions in view of controlling the anatase content in suspension plasma sprayed deposits.

Roman Jaworski, Lech Pawlowski, and **Agnès Le Maguer**, Service of Thermal Spraying at Ecole Nationale Supérieure de Chimie de Lille, BP 90108, 8, avenue Mendeleïev, Villeneuve d'Ascq 59652, France; **Francine Roudet**, Laboratory of Mechanics Lille, URM CNRS 8107, IUT A, BP 179, rue de la Recherche, Villeneuve d'Ascq 59653, France; and **Stefan Kozerski**, Faculty of Mechanics, Wroclaw University of Technology, ul. Lukasiewicza 5, 50-371 Wroclaw, Poland. Contact e-mail: lech.pawlowski@ensc-lille.fr.

2. Experimental

2.1 Suspensions Preparation and Injection

In the experiments, suspensions were formulated with the use of rutile TiO_2 (*Tioxide R-TC90* of *Huntsman Tioxide*) in the following proportions: 360 g of distilled water + 40 g of rutile + 0.12 g of dispersant. The dispersant was an aqueous solution of sodium polyacrylate (*Hydropalat N, Congis*). The size distribution of TiO_2 powder used in the suspension formulation is shown

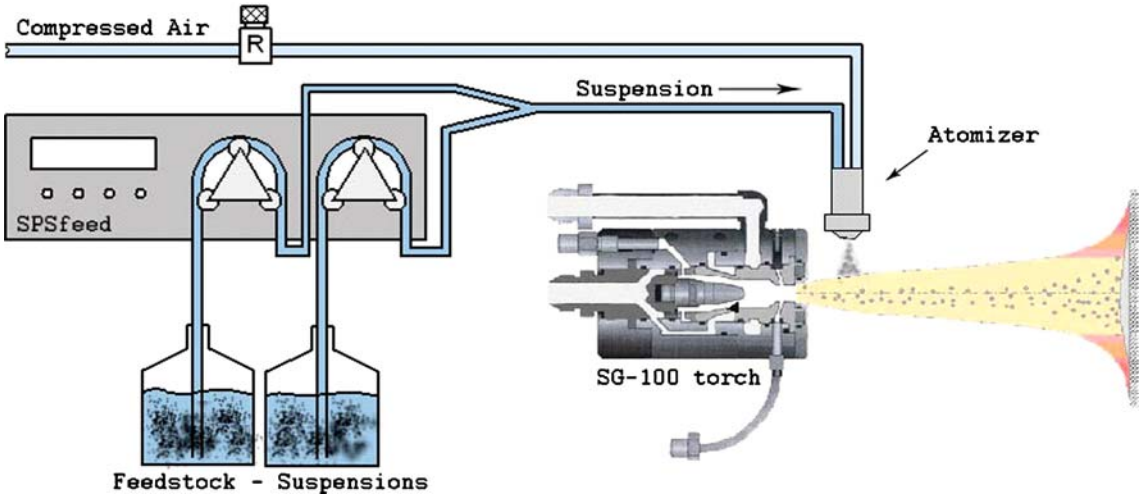

Fig. 1 Sketch of suspension plasma spraying

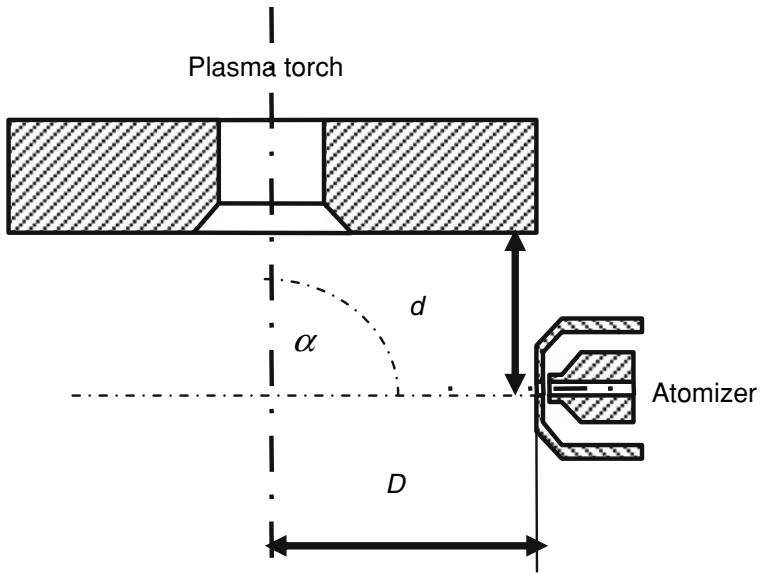

Fig. 2 Sketch of suspension injector. The ID of the atomized liquid delivery outlet is 1.5 mm and the ID of the suspension delivery outlet is 0.7 mm

elsewhere (Ref 11). The mean diameter (volume-surface mean defined by Masters (Ref 13)) equals to $d_{VS} = 0.33$ μm. The geometry of atomizer/injector is shown in Fig. 2. The parameters related to the suspension delivery are summarized in Table 1.

2.2 Plasma Spraying

Aluminum plates of size 15 × 15 × 3 mm were used as coatings substrates. They were plasma sprayed using *Praxair SG-100* torch with anode 03083-175 and cathode 03083-129 mounted on 5-axis *ABB IRB-6* industrial robot. Throughout all the experiments the following parameters were kept constant:

Table 1 Operational parameters related to injection

Variable	Value and unit
Atomizing gas	Air
Atomizationon gas pressure	0.6 bar
Angle of injection	90°
Distance *d*, mm	13
Distance *D*, mm	15

- composition of plasma working gas: $Ar + H_2$;
- flow rates of plasma working gas: $q_{Ar} = 45$ slpm and $q_{H_2} = 5$ slpm;
- linear torch velocity: v = 500 mm/s;

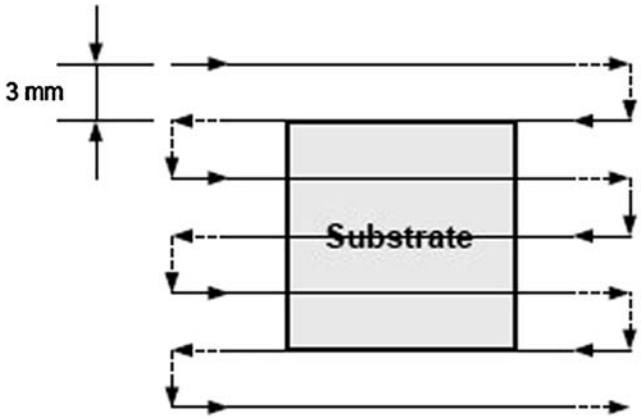

Fig. 3 Trajectory of the torch over the substrate

Table 2 Boundaries of the experimental space including low and high level values of variables

Variable	Spray process parameter	Low level $X_i = -1$	Central point $X_i = 0$	High level $X_i = +1$
X_1	Suspension feed rate, mL/min	20	30	40
X_2	Spray distance, cm	8	10	12
X_3	Power input to plasma, kW	38	39	40

- trajectory of one torch pass is presented in Fig. 3
- total number of passes was 50 (5 cycles of 10 passes including 1 min of cooling down).

The variable spray parameters, called experimental domain, are collected in Table 2. The full matrix of 2^3 experiments was realized for samples sprayed using water suspension and two experiments were made in the center. All experiments done are summarized in Table 3.

2.3 Powders and Coatings Characterization

Morphology of powders, splats and coatings surfaces and cross-sections was investigated using *JEOL-JSM 6480L* microscope, equipped with a detector of secondary electrons and an energy dispersive spectrometer (EDS). The cross-sections were prepared metallographically. Cameca *CAMEBAX* electron probe micro-analyzer was used for qualitative chemical analysis of sprayed coatings. The cross-sections of the sprayed samples were visualized using an optical microscope *Olympus CK 40 M* with a camera *Camedia 3040*. The thicknesses of the coatings were determined using software *DP-SOFT 5.0*. XRD analysis of powders and coatings was carried out using *Bruker* diffractometer of type D8 using Cu Kα radiation. The phases were identified with use of *Diffrac^{plus} EVA* software which uses database of International Centre of Diffraction Data JCPDS-ICDD.

2.4 Crystallographic Analyses

Initially, five mixtures of anatase and rutile powders were prepared. Rutile was the fine powder used in the suspensions and anatase was a 99.8% pure product of *Aldrich.* Their composition is shown in Table 4. Subsequently, the X-ray diagrams of the mixtures were realized and the content of anatase was determined from the following equation (Ref 14):

$$C_A = \frac{8I_A}{13I_R + 8I_A} \quad \text{(Eq 1)}$$

in which I_A is intensity of [101] peak of anatase and I_R is intensity of [110] peak of rutile. This expression was corrected by taking into account different densities of two phases of TiO_2 in the following way:

$$C_{Acor} = \frac{8I_A/\rho_A}{13I_R/\rho_R + 8I_A/\rho_A} \quad \text{(Eq 2)}$$

in which ρ_A is the density of anatase (3.9 g/cm^3) and ρ_R is the density of rutile (4.2 g/cm^3). The calculation was made by taking into account the heights and the areas of peaks and their results are shown in Table 5. The comparison of the methods enabled to retain the analysis of peaks heights with the corrections shown in Eq 2. The crystal

Table 3 Matrix 2^3 of plasma spraying experiments using water-based suspension (samples T1-T8) with two experiments in the center (samples T9 and T10)

Experiment no.	X_1	X_2	X_3
T1	−1	−1	−1
T2	1	−1	−1
T3	−1	1	−1
T4	1	1	−1
T5	−1	−1	1
T6	1	−1	1
T7	−1	1	1
T8	1	1	1
T9	0	0	0
T10	0	0	0

Table 4 Composition of powders mixtures for crystallographic investigations

wt.% of anatase	wt.% mass of rutile
100	0
75	25
50	50
25	75
0	100

Table 5 Comparison of determination the content of anatase (in wt.%) by different methods

Mechanical mixtures C_A of mixture	Analysis of peaks in X-ray diagrams			
	Heights of peaks		Areas of peaks	
	C_A (Eq 1)	C_{Acor} (Eq 2)	C_A (Eq 1)	C_{Acor} (Eq 2)
0.25	0.21	0.22	0.20	0.21
0.50	0.39	0.41	0.39	0.41
0.75	0.73	0.75	0.73	0.75

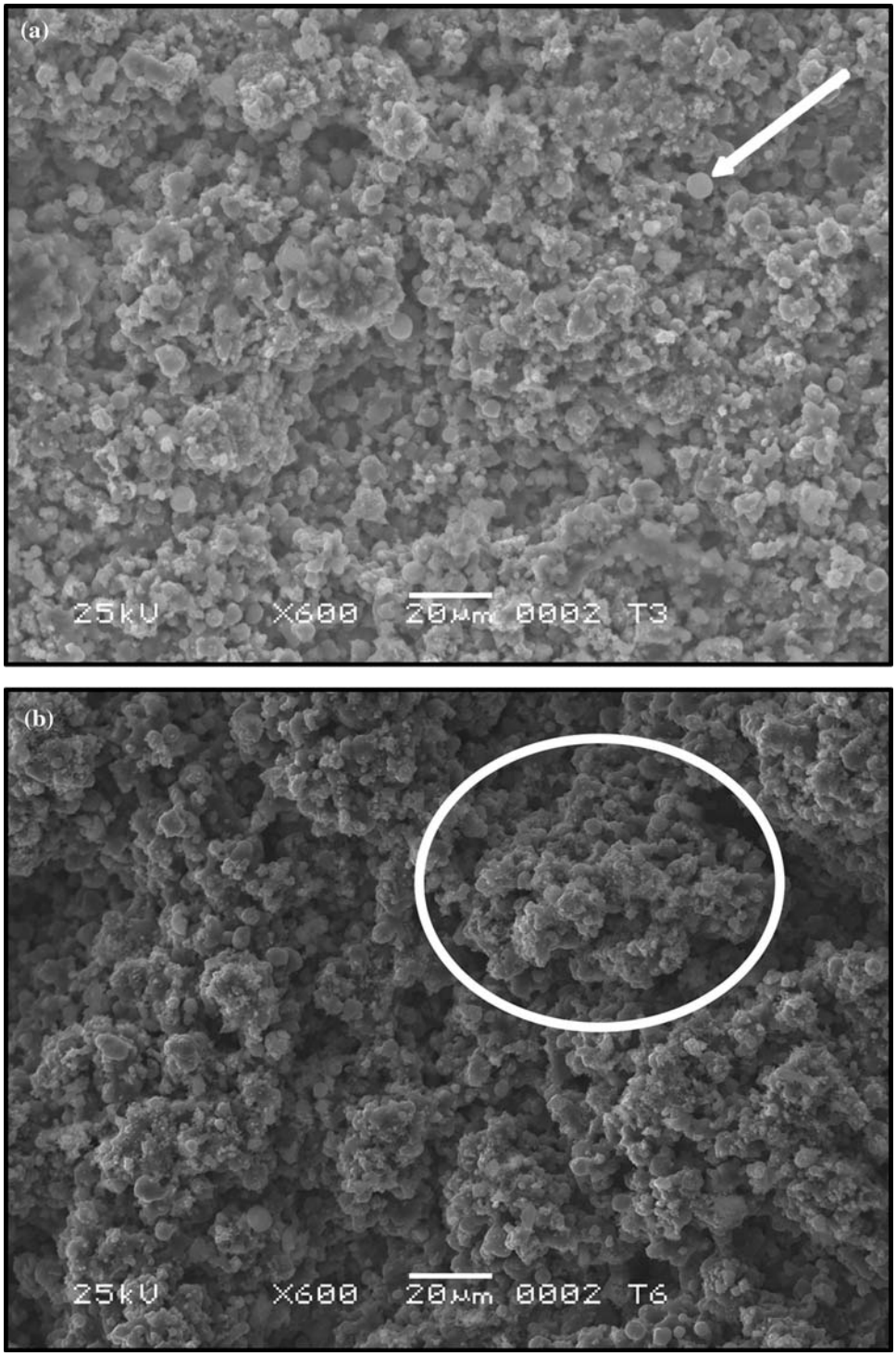

Fig. 4 SEM micrographs (secondary electrons) of some suspension plasma sprayed TiO_2 coatings surfaces: experiment T3-(a) and experiment T6-(b). Arrows indicate small particles rounded by fusion at flight in plasma and circles are made around bigger agglomerates of small particles

sizes were calculated from broadening of Bragg peaks using Laue-Scherer method. The influence of microstrains was taken into account in the way described elsewhere (Ref 15).

2.5 Statistical Treatment of Data

Optimization of operational spray parameters was made using three responses, namely:

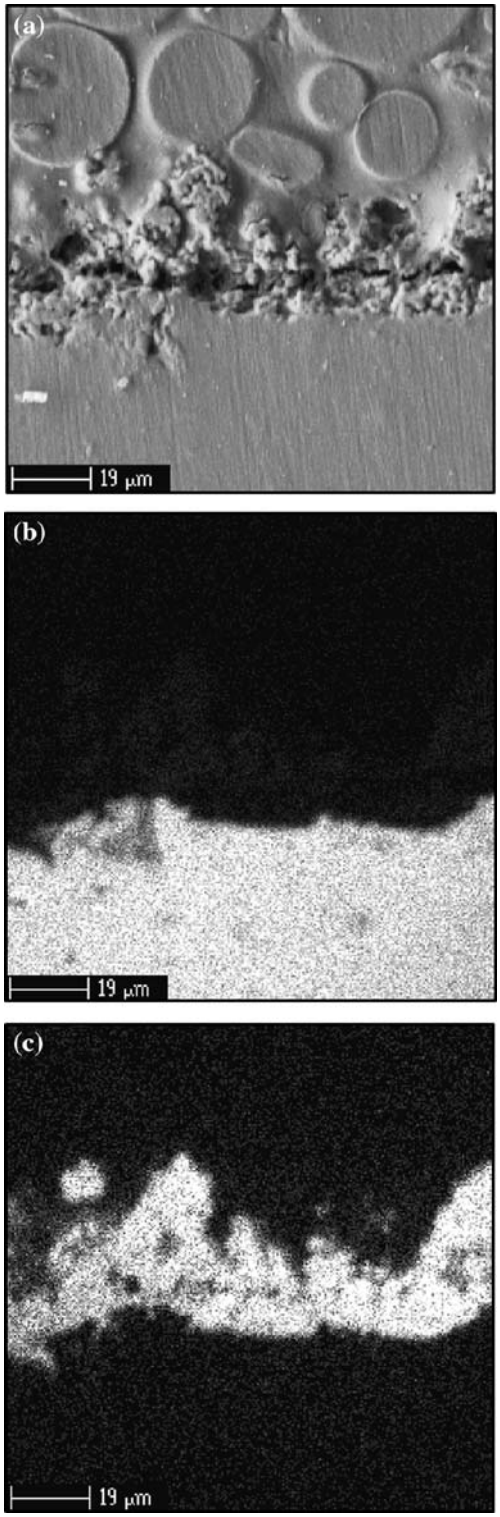

Fig. 5 SEM micrograph (secondary electrons) of the sample T9 cross-section (a); elements mapping of Al (b); and Ti (c)

- fraction of anatase phase in the coating, Y_1;
- coating thickness, Y_2;
- size of anatase crystals, Y_3.

The effects of the process variables onto responses were calculated following to the model valid in the experimental space[1]:

$$Y_m = b_0 + \sum b_i X_i + \sum b_{ij} X_i^* X_j + b_{123} X_1^* X_2^* X_3 \quad \text{(Eq 3)}$$

where i, j, k are equal to 1, 2, 3 and m can be equal 1, 2, or 3. The coefficient b_0 is the mean of responses of all experiments; b_i coefficient represents the effect of the variable X_i, and b_{ij} and b_{123} are the coefficients which represent the effects of interactions of variables $X_i{*}X_j$ and $X_1{*}X_2{*}X_3$, respectively. Experiments were carried out by considering a 2^3 full factorial design with two levels and three factors, i.e. a total of 8 experiments (Table 3). The advantage of this type of experimental design is that the structure is perfect for estimating the model (Eq 3). The analyzes were made using *Nemrod* software (Ref 16). They aimed at determination of significant (active) effects influencing quantitative properties of sprayed deposits. The method of statistical analyzes was a creation of the regression equation describing the property and an analysis of the coefficients of this equation. Initially, all effects and their first and second order interaction (as shown in Eq 3) were considered. Then the most active effects and their interactions were selected by application of the *Student* criterion. The selected coefficients should be greater than the incertitude calculated using reproducibility variance and *Student* criterion, taken at 95% confidence level and for a degree of freedom that depends, in turn, on number of experiments, number of their repetition, and on the number of regression equation coefficients as shown by Lazić (Ref 17). Later on, the analysis was repeated by taking only these effects in the regression equation into account (and narrowing the incertitude in coefficients determination). Finally, the probability that the effect is active was calculated with the use *Bayes* approach and the final statistical model of the analyzed property was established.

3. Results

3.1 Scanning Electron Microscope

The surfaces of the sprayed samples are presented in Fig. 4. The coatings include submicrometer and micrometer fine particles. Some of them are irregular and some are spherical (see arrows in Fig. 4). Careful analysis enables a distinction of greater agglomerates having size of a few tens of micrometers (see circle in Fig. 4). Such agglomerates are visible rather on the surface of coatings sprayed at greater distance of 12 cm and/or greater suspension flow rate of 30 mL/min. The energy dispersive spectroscopy analysis carried out for the samples T2, T3, T4, and T6 enabled qualitatively only Ti and O to be

[1]Defined as $-1 \le X_i \le +1$, $i = 1$ to 3, variables are normalized with regard to spray parameters in such a way that $X_i = -1$ corresponds to the lower limit of variable, $X_i = 0$ corresponds to the center of experimental domain and $X_i = 1$ corresponds to higher limit of the variable.

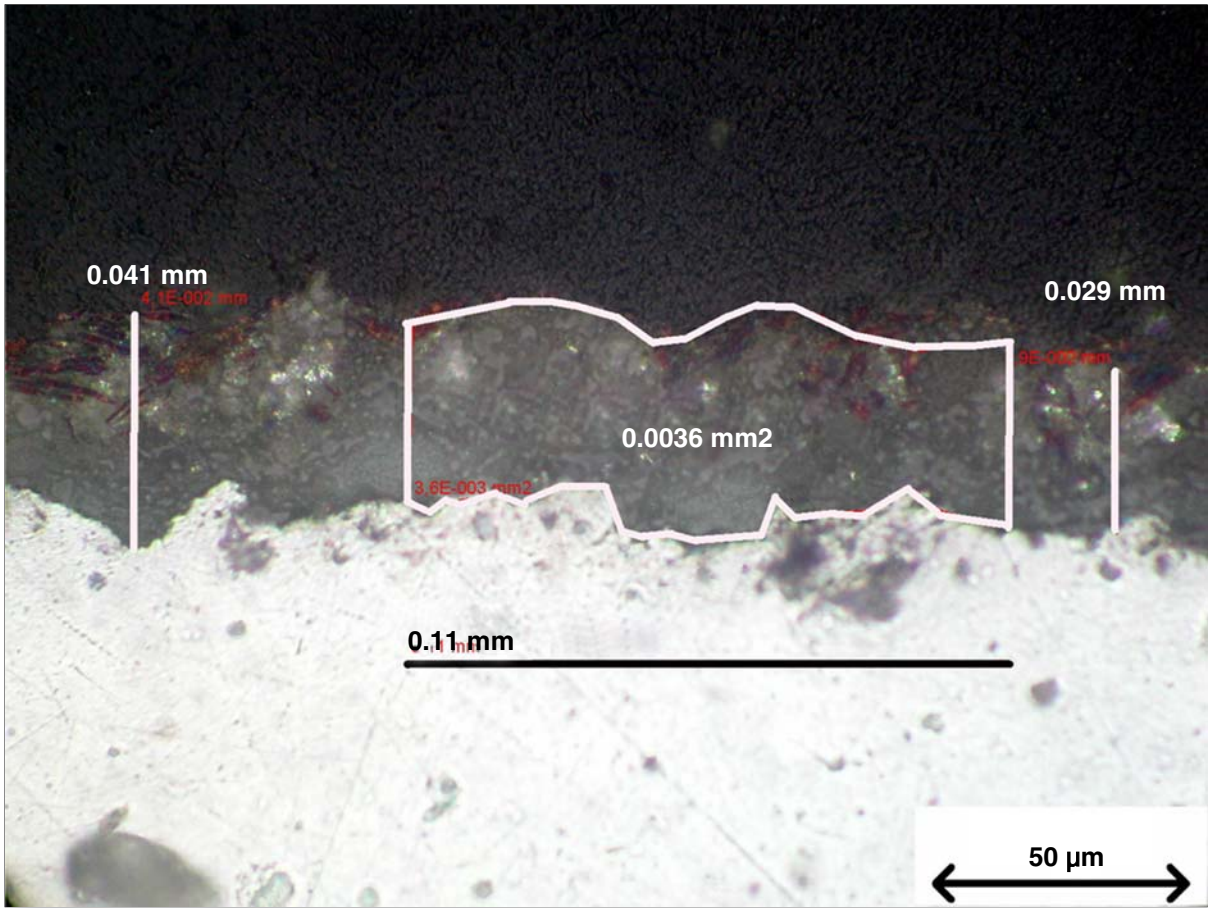

Fig. 6 Optical micrograph of the sample T2 cross-section with the details of thickness determination

Table 6 Measurements of thickness, fraction of anatase and size of anatase crystals in suspension sprayed coatings

Experiment no.	Thickness, µm	Fraction of anatase, wt.%	Size of anatase crystals, nm
T1	29	9.4	95
T2	33	11.8	97
T3	11	13.8	105
T4	22	15.3	89
T5	8	9.7	85
T6	10	9.9	82
T7	10	15.4	98
T8	9	14.5	82
T9	...	13.1	...
T10	...	12.1	...

discovered. The quantitative analysis made for the samples T2 and T4 enabled to find the atomic proportion of these elements of 66.7 at.% O and 33.3 at.% Ti, that corresponds to stoichiometric TiO_2. The secondary electron image of sprayed samples indicates an important porosity of the samples (Fig. 5a). The visible porosity could have resulted from the real porosity and from the *pull-out* effect at the metallographical preparation of the cross-sections.

3.2 Electron Micro-probe Mapping, Optical Microscope

The elementary mapping of Al and Ti made using EMPA technique shows sharp interface and important roughness of sprayed samples (Fig. 5b, c). Optical microscope investigation of a cross section of a coating confirms porosity and roughness of sprayed coatings (Fig. 6). The thicknesses of the coatings were calculated by averaging the thicknesses along a line. The results of the measurements are collected in Table 6.

3.3 Statistical Analyses

3.3.1 Fraction of Anatase in Deposits. The initial analysis shows that only coefficient b_2 is greater that the 95% significance level (Fig. 7a). The refined analysis with the regression equation limited to three principal variables and one interaction, i.e. $X_1{*}X_3$, shows that the interaction effect b_{13} is slightly greater than the signification level (Fig. 7b). However, the probability that the b_{13} interaction effect is smaller than 50% (see Fig. 7c) and the final regression equation has the following forms:

$$Y_1 = 12.5 + 2.3X_2 \quad \text{(Eq 4)}$$

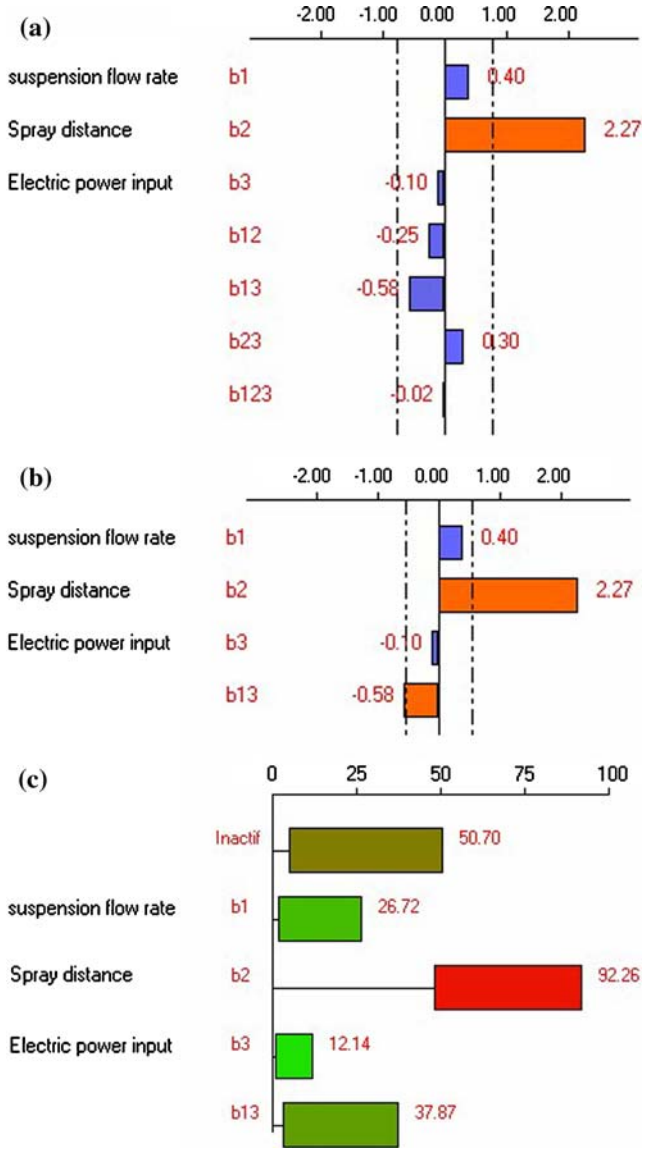

Fig. 7 Statistical analysis of the active effects influencing anatase fraction in sprayed deposits: regression equation coefficients for a model including all effects and their interaction of second and third order (a); refined regression equation coefficients for most active effects (b); determination of probability that the effects in the refined regression equation are active (c)

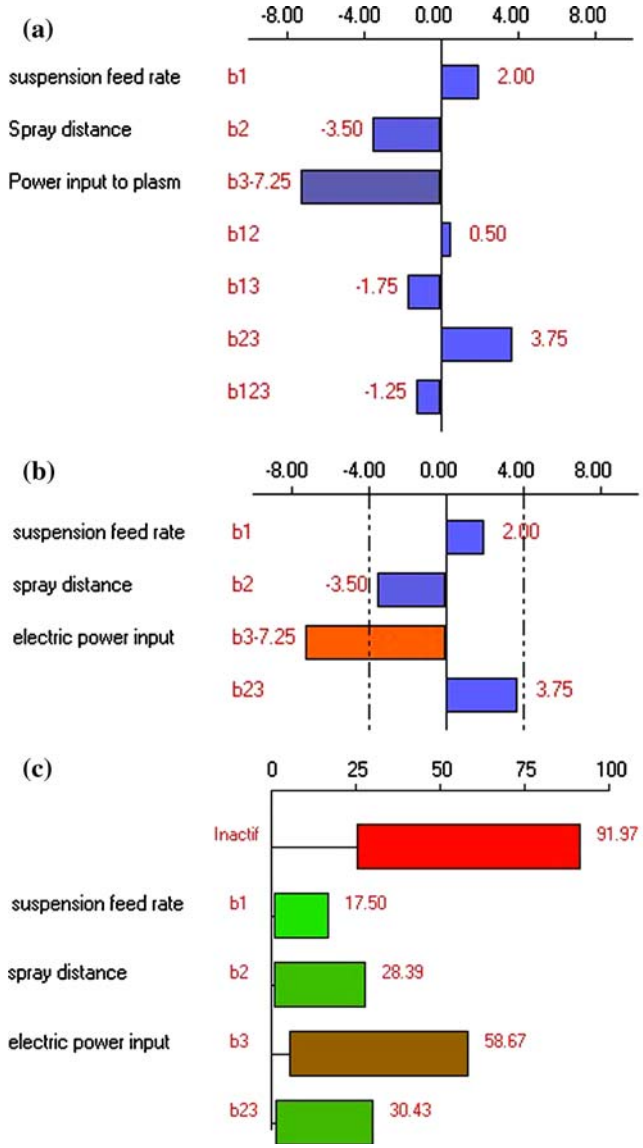

Fig. 8 Statistical analysis of the active effects influencing coating thickness: regression equation coefficients for a model including all effects and their interaction of second and third order (a); refined regression equation coefficients for most active effects (b); determination of probability that the effects in the refined regression equation are active (c)

3.3.2 Coating Thickness. Initial analysis indicates that no coefficient of the regression equation is greater than 95% significance level (Fig. 8a). The analysis limited to three principal effects and $X_2{*}X_3$ interaction enabled to find out that the effect b_3 of electric power input to plasma is significant what was confirmed by the probability calculation (Fig. 8b, c)

$$Y_2 = 16.5 - 7.3X_3 \quad \text{(Eq 5)}$$

3.3.3 Anatase Crystal Size. Similarly, initial analysis does not reveal any significant effect and refined analysis indicates that b_1, b_3, and b_{12} can be significant (Fig. 9a, b). The probability that these effects are active is lower than 50% (Fig. 9c). Consequently, it is probable that no significant effect of chosen variables influences anatase crystal size.

4. Discussion

The droplets of atomized liquid are injected into plasma jet. Knowing that the size of suspension delivery outlet is 700 μm (see Fig. 2) and that the liquid is subsequently

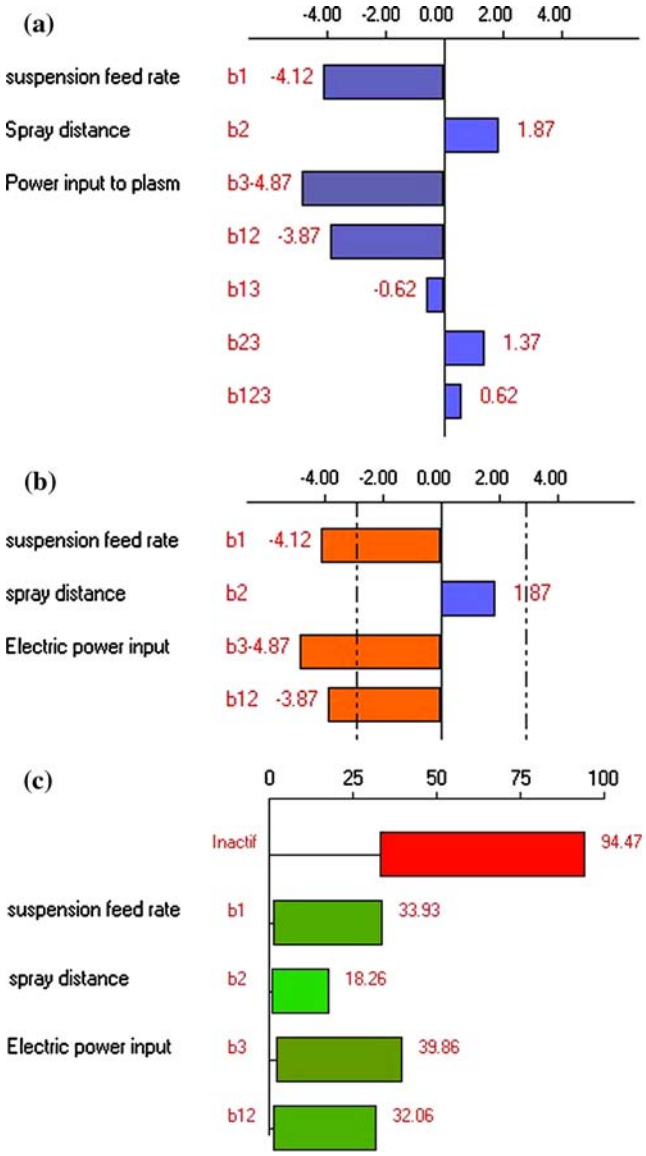

Fig. 9 Statistical analysis of the active effects influencing anatase crystal size in sprayed deposits: regression equation coefficients for a model including all effects and their interaction of second and third order (a); refined regression equation coefficients for most active effects (b); determination of probability that the effects in the refined regression equation are active (c)

Table 7 Estimation of solid TiO_2 particles content in the droplets of used suspension liquid having size of 50 and 500 μm

Data of suspension liquid and solid content of TiO_2	50 μm droplet	500 μm droplet
Volume of droplet, cm^3	6.5×10^{-5}	6.5×10^{-8}
Mass of TiO_2, g	7.3×10^{-9}	7.3×10^{-6}
Diameter of rutile agglomerates corresponding to the mass, μm	16	150
Number of rutile particles of a mean size of 0.33 μm in a droplet	About 100,000	About 92 millions

atomized, the sizes of droplets must have diameter ranging from a few tens to a few hundreds of micrometers. The droplets are accelerated in the plasma jet and disintegrated into smaller droplets. Simultaneously, water boils and gets evaporated. The solid particles inside any droplet get closer and may start to agglomerate by sintering in flight. The number of solid particles in the droplets is estimated in Table 7. The process can be compared to that of spray-drying described by Masters (Ref 13). However, the processes have the following, significant differences:

- particularly hot heating medium (plasma jet);
- boiling of suspension liquid;
- very short heating time (milliseconds instead of seconds);
- missing of a binder in the liquid.

The rough estimation of the number of small particles in suspension droplets of different sizes is shown in Table 7. A part of precursor gets molten in the initial part of their trajectory. Fauchais et al. (Ref 10) estimated that the precursors having size of 0.1 μm gets molten after 2.5 mm of its trajectory in the plasma jet. In fact, the plasma gets colder because of evaporation of water and the trajectory may be longer. Subsequently, the fine particles may get agglomerated by sintering with other particles and/or evaporated. The agglomeration progresses until an impact with the substrate. This can be confirmed by aspect of surface of the coatings sprayed using greater spray distance, which has slightly more agglomerates visible (Fig. 4). As the atmosphere around solid precursors contains a lot of vapours of water the solidification of precursors in-flight is probable. Anatase has lower interfacial energy between liquid and solid TiO_2 and this phase is likely to nucleates firstly (Ref 12). Moreover, the cooling of a precursor in flight is very rapid and anatase is likely to be formed in its entire volume because of their small size. An increase of anatase phase fraction with the spray distance can be attributed to the increasing number of solidified precursors arriving on the substrate. The precursors being molten at impact with substrate nucleates as anatase but this phase can transform back to rutile on cooling of the coating. This transformation is more probably for larger agglomerates due to the larger quantity of heat of fusion liberated and lower cooling rate. As the size of anatase and rutile crystals, being about 100 nm (see Table 6) is comparable to the size of particles, it is reasonable to suppose that the particles are entirely rutile or entirely anatase. The anatase-particles are generated in flight and rutile-particles are unmelted ones and those, which transform back from anatase-particles when the coating cools down.

Thickness of the coatings depends mainly on power input to plasma. An increase in electric power input results in a decrease of thickness. It can be explained by an increase of velocity of plasma stream with electric power input to plasma. The stream generated with increasing electric power input to the torch is more rapid and more turbulent. Such a stream is likely to blow away these

particles, which are not closely adhering to the substrate or to previously deposited coating.

5. Conclusions

A statistical study was carried out to find out the influence of operational spray parameters of TiO_2 on coatings thickness and on some microstructural features such as fraction of anatase in the coatings and the crystal size. The spray distance has most probably the strongest influence on the anatase fraction in coatings. The phenomenon was explained by an increase of number of fine particles solidified in flight before an impact with substrate. The electric power input to the torch was probably influencing thickness of suspension plasma sprayed coatings. The influence of other parameters on tested coatings characteristics was not significant. Further studies are carried out aiming at testing of other solutions formulation and its injection into plasma jet.

Acknowledgments

Ms. Ophelie Meunier, Maria Aguila, and Mr. Christophe Penverne of ENSCL helped in X-ray diffraction studies of samples. Professors Didier Chicot and Jacky Lesage made SEM installation available.

References

1. L. Pawlowski, Dépôts Physiques. PPUR, Lausanne, Switzerland, 2003
2. L. Pawlowski, The Science and Engineering of Thermal Spray Coatings, 2nd ed., John Wiley & Sons, Chichester, England, 2008
3. F.-L. Toma, G. Bertrand, S.-O. Chwa, C. Coddet, D. Klein, P. Nardin, and A. Ohmori, Studies of the Photocatalytic Efficiency of Titanium Dioxide Powders and Coatings Obtained by Plasma Spraying, *Conference Proceedings on CD-ROM, ITSC 2004*, Osaka, Japan, May 10-12, 2004, DVS Verlag, Düsseldorf, Germany
4. F.-X. Ye, A. Ohmori, and C.-J. Xi'an, The Photoresponse and Donor Concentration of Plasma Sprayed TiO_2 and TiO_2-ZnO Electrodes, *Conference Proceedings on CD-ROM, ITSC 2004*, Osaka, Japan, May 10-12, 2004, DVS Verlag, Düsseldorf, Germany
5. F.-L. Toma, G. Bertrand, D. Klein, L.-M. Berger, and S. Thiele, Photocatalytic Properties of Coatings Sprayed from TiO_x and $Ti_{n-2}Cr_2O_{2n-1}$ Powders by APS and VPS, *Conference Proceedings on CD-ROM, ITSC 2004*, Osaka, Japan, May 10-12, 2004, DVS Verlag, Düsseldorf, Germany
6. F.-L. Toma, G. Bertrand, D. Klein, C. Coddet, and C. Meunier, Photocatalytic Decomposition of Nitrogen Oxides Over TiO_2 Coatings Elaborated by Liquid Feedstock Plasma Spraying, *Conference Proceedings on CD-ROM, ITSC 2005*, Basel, Switzerland, May 2-4, 2005, DVS Verlag, Düsseldorf, Germany
7. J. Karthikeyan, C.C. Berndt, S. Reddy, J.-Y. Wang, A.H. King, and H. Herman, *J. Am. Ceram. Soc.*, 1998, **81**(1), p 121-128
8. T. Bhatia, A. Ozturk, L. Xie, E.H. Jordan, M. Gell, X. Ma, and N.P. Padture, *J. Mater. Res.*, 2002, **17**(9), p 2363-2372
9. N.P. Padture, K.W. Schichting, T. Bhatia, A. Ozturk, B. Cegeten, E.H. Jordan, M. Gell, S. Jiang, T.D. Xiao, P.R. Strutt, E. Garcia, P. Miranzo, and M.I. Osendi, *Acta Mater.*, 2001, **49**, p 2251-2257
10. P. Fauchais, J.F. Coudert, V. Rat, J. Fazilleau, and C. Delbos, *1st International Meeting on Thermal Spraying*, Lille, ed. L. Pawlowski, 4-5 December 2003, p 8-13
11. R. Tomaszek, L. Pawlowski, L. Gengembre, J. Laureyns, Z. Znamirowski, and J. Zdanowski, *Surf. Coat. Technol.*, 2006, **201**, p 45-56
12. Y. Li and T. Ishigaki, *J. Cryst. Growth*, 2002, **242**, p 511-516
13. K. Masters, Spray Drying Handbook, 4th ed., George Godwin, London, England, 1985, p 67
14. N. Berger-Keller, G. Bertrand, C. Filiatre, C. Meunier, and C. Coddet, *Surf. Coat. Technol.*, 2003, **168**, p 281-290
15. V. Deram, C. Minichiello, R.N. Vannier, A. Le Maguer, L. Pawlowski, and D. Murano, *Surf. Coat. Technol.*, 2003, **166**, p 153-159
16. *Nemrod*, software, version Education 2000 (Marseille, France), LPRAI
17. Ž.R. Lazić, Design of Experiments in Chemical Engineering. Wiley-VCH, Weinheim, Germany, 2004, p 262-385